EC Journals.ASM.org

Resolving Phenylalanine Metabolism Sheds Light on Natural Synthesis of Penicillin G in *Penicillium chrysogenum*

Tânia Veiga,[a,c] Daniel Solis-Escalante,[a,c] Gabriele Romagnoli,[a,c] Angela ten Pierick,[b,c] Mark Hanemaaijer,[b,c] Amit Deshmuhk,[b,c] Aljoscha Wahl,[b,c] Jack T. Pronk,[a,c] and Jean-Marc Daran[a,c]

Industrial Microbiology Section, Department of Biotechnology, Delft University of Technology, Julianalaan 67, 2628 BC Delft, The Netherlands[a]; Bioprocess Technology Section, Department of Biotechnology, Delft University of Technology, Julianalaan 67, 2628 BC Delft, The Netherlands[b]; and Kluyver Centre for Genomics of Industrial Fermentation, P.O. Box 5057, 2600 GA Delft, The Netherlands[c]

The industrial production of penicillin G by *Penicillium chrysogenum* requires the supplementation of the growth medium with the side chain precursor phenylacetate. The growth of *P. chrysogenum* with phenylalanine as the sole nitrogen source resulted in the extracellular production of phenylacetate and penicillin G. To analyze this natural pathway for penicillin G production, chemostat cultures were switched to [U-^{13}C]phenylalanine as the nitrogen source. The quantification and modeling of the dynamics of labeled metabolites indicated that phenylalanine was (i) incorporated in nascent protein, (ii) transaminated to phenylpyruvate and further converted by oxidation or by decarboxylation, and (iii) hydroxylated to tyrosine and subsequently metabolized via the homogentisate pathway. The involvement of the homogentisate pathway was supported by the comparative transcriptome analysis of *P. chrysogenum* cultures grown with phenylalanine and with $(NH_4)_2SO_4$ as the nitrogen source. This transcriptome analysis also enabled the identification of two putative 2-oxo acid decarboxylase genes (Pc13g9300 and Pc18g01490). cDNAs of both genes were cloned and expressed in the 2-oxo-acid-decarboxylase-free *Saccharomyces cerevisiae* strain CEN.PK711-7C (*pdc1 pdc5 pdc6*Δ *aro10*Δ *thi3*Δ). The introduction of Pc13g09300 restored the growth of this *S. cerevisiae* mutant on glucose and phenylalanine, thereby demonstrating that Pc13g09300 encodes a dual-substrate pyruvate and phenylpyruvate decarboxylase, which plays a key role in an Ehrlich-type pathway for the production of phenylacetate in *P. chrysogenum*. These results provide a basis for the metabolic engineering of *P. chrysogenum* for the production of the penicillin G side chain precursor phenylacetate.

The interest in *Penicillium* as an antibiotic producer started with the discovery of penicillin by Fleming (20). The recognition of the therapeutic value of penicillin (9) led to intensive research to increase productivity. This research involved strain improvement as well as the extensive optimization of process conditions and growth media (5, 50, 52, 57, 59, 66, 69). Growth in complex media was found to promote the synthesis of a wide range of β-lactam antibiotics (8), including benzylpenicillin (now commonly known as penicillin G).

Penicillin G is the predominant type of penicillin produced in *P. chrysogenum* cultures supplemented with corn steep liquor (50, 51). The analysis of penicillin G degradation products revealed the release of phenylacetate (11, 52), and the incorporation of phenylacetate in penicillin G was confirmed by labeling studies with deuterated phenylacetyl-N_6'-DL-valine and [^{14}C]phenylacetate (4, 25). The addition of phenylacetate to the culture broth was shown to lead to substantially increased penicillin yield and productivity (52). Since then, the addition of the side chain precursor phenylacetate has been an integral part of industrial fermentation processes for the production of penicillin G with *P. chrysogenum*.

Instead of being incorporated in penicillin G, phenylacetate also can be oxidized into 2-hydroxyphenylacetate and catabolized to acetoacetate and fumarate via the homogentisate pathway (2, 17–19, 46). This enables some ascomycetous fungi (e.g., *Aspergillus nidulans* and *Penicillium notatum*) to grow on phenylacetate (17, 61, 62). Although *P. chrysogenum* cannot grow on phenylacetate as the sole carbon source, it can efficiently oxidize it (61). This ability has been severely reduced in modern production strains, which preferentially incorporate phenylacetate to penicillin G instead of catabolizing it (26, 72). In contrast to the *P. chrysogenum* NRRL 1951 strain, which is the ancestor of modern penicillin-producing strain lineages, the model strain Wisconsin 54-1255, which represents an early stage in strain improvement, already exhibits the reduced consumption of phenylacetate and stable penicillin G production. This phenotype was correlated with a point mutation ($598^{C\rightarrow T}$) in the *pahA* gene that encodes phenylacetate hydroxylase (61, 62).

While the fate of phenylacetate added to *P. chrysogenum* cultures has been extensively studied (26, 51, 52, 61, 62), the pathways responsible for the natural production of penicillin G by this fungus have scarcely been investigated. The metabolism of aromatic compounds in filamentous fungi presents a high degree of metabolic diversity. Several biochemical studies showed that, in ascomycetous fungi, phenylacetate is an intermediate of phenylalanine catabolism (35, 47–49). [^{14}C]L-phenylalanine tracer experiments in *Aspergillus niger* showed that L-phenylalanine metabolism yielded metabolites such as phenylacetate, 2- and 4-hydroxyphenylacetate, and homogentisate, as well as 4-hydroxymandelate and protocatechuate. Interestingly and in contrast to findings for human metabolism, labeled tyrosine was not de-

Received 3 November 2011 **Accepted** 2 December 2011
Published ahead of print 9 December 2011
Address correspondence to J.-M. Daran, j.g.daran@tudelft.nl.
Supplemental material for this article may be found at http://ec.asm.org/.

doi:10.1128/EC.05285-11
The authors have paid a fee to allow immediate free access to this article.

TABLE 1 *S. cerevisiae* and *P. chrysogenum* strains used in this study

Strain	Genotype	Reference
S. cerevisiae		
CEN-PK711-7C	*MAT***a** *MAL2-8c SUC2 ura3 pdc1*Δ*pdc5*Δ*pdc6*Δ*aro10*Δ*thi3*Δ	74
CEN-PK113-5D	*MAT***a** *MAL2-8C SUC2 ura3*	74
IMZ001	*MAT***a** *MAL2-8c SUC2 ura3 pdc1*Δ*pdc5*Δ*pdc6*Δ*aro10*Δ*thi3*Δp426GPD(*URA3*)	74
IMZ002	*MAT***a** *MAL2-8c SUC2 ura3 pdc1*Δ*pdc5*Δ*pdc6*Δ*aro10*Δ*thi3*ΔpUDE001(*URA3 TDH3p-ARO10*)	74
IME004	*MAT***a** *MAL2-8c SUC2* p426GPD(*URA3*)	74
IMZ245	*MAT***a** *MAL2-8c SUC2 ura3 pdc1*Δ*pdc5*Δ*pdc6*Δ*aro10*Δ*thi3*ΔpUDE98(*URA3 TDH3p-Pc13g09300*)	This study
IMZ246	*MAT***a** *MAL2-8c SUC2 ura3 pdc1*Δ*pdc5*Δ*pdc6*Δ*aro10*Δ*thi3*ΔpUDE99(*URA3 TDH3p-Pc18g01490*)	This study
P. chrysogenum		
DS17690	High penicillin producer	26

tected, suggesting the absence of a functional phenylalanine hydroxylase (35). In basidiomycetes (e.g., *Schizophyllum commune*), phenylalanine also can be catabolized through the phenylpropanoid pathway, in which phenylalanine is converted into cinnamate by a phenylalanine ammonia lyase (47–49).

Currently the phenylacetate added as a side chain precursor for penicillin production is derived from petrochemical raw materials (64). An understanding of natural pathways for the production of phenylacetate and penicillin G by *P. chrysogenum* is required to explore metabolic engineering strategies from the complete *de novo* synthesis of penicillin G from renewable materials. Moreover, such knowledge may stimulate research into the role and regulation of penicillin biosynthesis in natural environments.

The goal of the present study was to gain insight into the mechanism of phenylacetate production in *P. chrysogenum*. ^{13}C-labeling experiments combined with metabolic network modeling, the analysis of intra- and extracellular product formation, and genome-wide expression profiling were used to investigate phenylalanine catabolism in chemostat cultures grown in the absence of added phenylacetate. Based on this systematic approach, two putative *P. chrysogenum* genes for 2-oxo-acid decarboxylase were identified and functionally characterized by expression in a 2-oxo-acid decarboxylase-negative *Saccharomyces cerevisiae* strain.

MATERIALS AND METHODS

Strains. The *P. chrysogenum* and *S. cerevisiae* strains used in this study are listed in Table 1. *P. chrysogenum* DS17690 is a penicillin high-producing strain, resulting from the DSM strain improvement program (3, 40, 55). Requests for the academic use of the *P. chrysogenum* strains used in this study, under a material transfer agreement, should be addressed to R. A. L. Bovenberg (DSM Biotechnology Center, Delft, The Netherlands). All *S. cerevisiae* strains were constructed in the CEN.PK background (16).

Strain construction. The Pc18g01490 and Pc13g09300 cDNAs were PCR amplified using a cDNA pool synthesized from total RNA isolated from *P. chrysogenum* DS17690, which was grown in glucose-limited chemostat cultures with phenylalanine as the nitrogen source, as the template. cDNA was synthesized using the GeneChip one-cycle cDNA synthesis kit (P/N 900431; Affymetrix, Santa Clara, CA) according to the manufacturer's recommendations. Pc18g01490 was PCR amplified with the primer pair Pc18g01490 fw + SpeI/Pc18g01490 rv + Xho (see Table S1 in the supplemental material), using Phusion Hot-Start polymerase (Finnzymes, Landsmeer, The Netherlands). The PCR product was cut with the restriction enzymes SpeI and XhoI and ligated into the plasmid p426GPD (53), which was previously digested with the same enzymes. The resulting plasmid was named pUDE98. Pc13g09300 was PCR amplified with the primer pair Pc13g09300 Gateway fw/Pc13g09300 Gateway rv (Table S1) using Phusion Hot-Start polymerase (Finnzymes). The PCR fragment then was recombined into pDNOR221 by BP clonase (Invitrogen, Breda, The Netherlands). The resulting vector, pEntry-Pc13g09300, then was recombined into pAG426-GPD (1) by LR clonase, resulting in the expression vector PUDE99. Both cDNAs were sequenced to verify the fidelity of the polymerase. The PCR products were sequenced by the Sanger method at Baseclear (Leiden, The Netherlands). The resulting sequences were compared to the sequences of *P. chrysogenum* Wisconsin 54-1255 (71) using Clustal W (38), revealing no mutation relative to the Wisconsin 54-1255 sequence. The coding sequences of Pc13g09300 and Pc18g01490 were deposited in GenBank under accession numbers JQ086348 and JQ086347, respectively. Plasmids pUDE98 and pUDE99 were transformed into *S. cerevisiae* CEN.PK711-7C, and the resulting strains were named IMZ246 (Pc18g01490) and IMZ247 (Pc13g09300), respectively (Table 1). *S. cerevisiae* strains were transformed using the lithium acetate single-stranded carrier DNA-polyethylene glycol method (22). Standard molecular biology methods were carried out as previously described (63).

Sequencing the DS17690 *pahA* allele. Genomic DNA of the *P. chrysogenum* strain DS17690 was isolated using the E.Z.N.A. fungal DNA kit (Omega Bio-tek, Amsterdam, The Netherlands). The *pahA* gene from *P. chrysogenum* DS17690 was PCR amplified from genomic DNA with the primers pair *pahA* Fw/*pahA* Rv (see Table S1 in the supplemental material). The PCR products were sequenced by the Sanger method at Baseclear (Leiden, The Netherlands), and sequences were compared to that of *P. chrysogenum* Wisconsin 54-1255 using Clustal W (38). The sequence has been deposited at GenBank (accession number JQ086346).

Chemostat cultivation. Carbon-limited chemostat cultures of *P. chrysogenum* were fed with a filter-sterilized carbon-limited defined mineral medium. Per liter of demineralized water, this medium contained 0.8 g KH_2PO_4, 8.75 g phenylalanine [$(NH_2)C_9H_9O_2$] or 5 g $(NH_4)_2SO_4$, 3.8 g Na_2SO_4, 0.5 g $MgSO_4 \cdot 7H_2O$, 7.5 g of glucose, and 10 ml of trace element solution. The trace element solution contained 15 g · liter^{-1} $Na_2EDTA \cdot 2H_2O$, 0.5 g · liter^{-1} $CuSO_4 \cdot 5H_2O$, 2 g · liter^{-1} $ZnSO_4 \cdot 7H_2O$, 2 g · liter^{-1} $MnSO_4 \cdot H_2O$, 4 g · liter^{-1} $FeSO_4 \cdot 7H_2O$, and 0.5 g · liter^{-1} $CaCl_2 \cdot 2H_2O$. KOH was added to set the medium pH at 5.5. In carbon-limited chemostat cultures of *P. chrysogenum* with $(NH_4)_2SO_4$ as the sole nitrogen source, penicillin G production was induced by the addition of 0.58 g · liter^{-1} of phenylacetate to the medium. Aerobic chemostat cultivation on nonlabeled substrates was performed in 3-liter bioreactors (Applikon, Schiedam, The Netherlands), with a working volume of 1.8 liters, at a dilution rate of 0.03 h^{-1} and at pH 6.5 as previously described (27), with the exception of the employed antifoam. The BDH (10%, vol/vol) antifoam (VWR International BV, Amsterdam, The Netherlands) was replaced by silicone antifoam (Bluestar Silicone, Lyon, France). The culture was decomposed in three phases: (i) an initial batch fermentation, (ii) a fed-batch phase between the start of the feed and the steady state, and (iii) the steady-state phase (12). Continuous cultures were assumed to be in steady state after at least 5 volume changes had passed since the last change

in cultivation conditions and when culture dry weight and off-gas CO_2 analyses differed by less than 4% for two consecutive volume changes.

Labeling experiments with L-[U-^{13}C]phenylalanine [$(NH_2)^{13}C_9H_9O_2$] (Cambridge Isotope Laboratories Inc., MA) were carried out in a 7-liter bioreactor (Applikon, Schiedam, The Netherlands), with a working volume of 4 liters, and maintained by a level controller and a dilution rate of 0.05 h^{-1}. The airflow rate was set at 2 liters · min^{-1} with a 0.3-bar overpressure. The mixing of the reactor content was accomplished with two six-bladed Ruston turbine impellers (diameter, 8 cm) operated at a rotation speed of 500 rpm. Foam formation was suppressed by the addition of approximately 70 $\mu l \cdot h^{-1}$ of antifoam agent BC86/013 (Basildon Chemicals, Abingdon, United Kingdom). The temperature of the reactor was kept at 25 ± 0.1°C by means of a thermocirculator, and the pH of the culture was maintained at 6.5 with 4 M NaOH by an automatic pH control system (Applikon Schiedam, The Netherlands). Dissolved-oxygen tension was monitored but not controlled, and it never dropped below 50% of air saturation during the course of the experiment. O_2 and CO_2 concentrations in the off gas were analyzed using a combined paramagnetic/infrared NGA 2000 MLT 1 gas analyzer (Fisher-Rosemount GMbH & Co, Hasselroth, Germany) (15, 54). After reaching steady state, the nonlabeled phenylalanine medium was switched to a chemically identical medium containing phenylalanine uniformly labeled on carbon as the sole nitrogen source.

S. cerevisiae was grown in glucose-limited chemostat cultures on a filter-sterilized defined mineral medium containing, per liter of demineralized water, the following: 3 g KH_2PO_4, 5 g phenylalanine [$(NH_2)C_9H_9O_2$] or 5g $(NH_4)_2SO_4$, 6.6 g K_2SO_4, 0.5 g $MgSO_4 \cdot 7H_2O$, 7.5 g of glucose, 1 ml of trace element solution, 1 ml of vitamin solution, and 8% antifoam-C emulsion (Sigma-Aldrich, Zwijndrecht, The Netherlands) (6). Trace element and vitamin solutions were prepared as described previously (73). The chemostat cultivation of *S. cerevisiae* was performed in 2-liter bioreactors (Applikon, Schiedam, The Netherlands) with a working volume of 1 liter and a dilution rate of 0.10 h^{-1}, as described previously (74). Continuous cultures were assumed to be in steady state after at least 5 volume changes and when the culture dry weight and off-gas CO_2 analyses differed by less than 2% for two consecutive volume changes.

Sampling for intracellular metabolite analysis. For intracellular metabolite measurements, approximately 1.2 ml of sample was withdrawn into 8 ml of 40% (vol/vol) aqueous methanol solution at −27.5°C, using a rapid sampling device, for the immediate quenching of the metabolic activity (15, 37). The sample then was washed 3 times with 20 ml of 40% (vol/vol) aqueous methanol via vacuum filtration, and the samples subsequently were stored at −27.5°C as previously described (13, 15). After the final methanol washing step for the steady-state samples, different amounts (120 and 300 μl) of a ^{13}C internal standard solution (0°C) were pipetted on top of the dry filter cake for accurate quantification by isotope dilution mass spectrometry (IDMS) (78). The metabolites then were extracted using 30 ml of 75% (vol/vol) ethanol-water at 73°C and subsequently kept in a water bath at 95°C for 3 min (24). The extracts were centrifuged at 4,600 rpm for 7 min and filtered (0.2 μm filter; FP30/0.2 CA-S; Whatman, Maidstone, England). Filtrates were placed in an evaporator (Labconco Corporation, Kansas City, MO) for 2.5 h at 30°C. The final volume was adjusted to 600 μl with Milli-Q water, and samples were flash frozen with liquid nitrogen and stored at −80°C until further analysis (15).

Sampling for extracellular metabolite analysis. For extracellular metabolite analysis, approximately 2 ml of broth was withdrawn from the bioreactor and immediately quenched with cold steel beads in a syringe (45) and filtered (0.45-μm-pore-size membrane filter). For steady-state samples, 20 μl of ^{13}C extract was added to 80 μl of this filtrate. Vials were immediately frozen with liquid nitrogen and stored (at −80°C) for further analysis.

Analysis of metabolites and isotopologues. Mass isotopomer distribution (MID) and concentration were measured using gas chromatography-mass spectrometry (GC-MS) as previously described (13). One hundred-μl samples were lyophilized and derivatized using 75 μl acetonitrile and 75 μl of N-methyl-N-(tertbutyldimethylsilyl) trifluoroacetamide (MTBSTFA; Thermo Scientific, Rockford, IL). Derivatized metabolites were obtained with fragment M-57 (see Table S2 in the supplemental material). The influence of derivatization agents and non-carbon atoms on the MID was corrected (76). The metabolite concentration was determined using IDMS with ^{13}C-labeled cell extract as an internal standard (45, 78). The metabolites phenylethanol and phenylethylamine did not show a peak in standards, while no standard was available for phenylacetaldehyde.

Glucose and phenylacetate concentrations in media and culture supernatant were measured by high-performance liquid chromatography (HPLC; Waters Alliance 2695 separation module supplied with a Waters 2487 dual absorbance detector and a Waters 2410 refractive index detector; Waters, Milford, MA) with a Bio-Rad HPX87H column (Bio-Rad, Hercules, CA). The mobile phase consisted of 0.5 mM, and the elution conditions were set at 60°C and at 0.6 ml · min^{-1} for the flow rate.

Penicillin G was measured on a Waters 2690 with a Zorbax column (Agilent, Amstelveen, The Netherlands) and a Waters 486 turnable absorbance detector (UV/VIS) at 30°C. The mobile phase consisted of 5 M acetonitrile, 5 mM KH_2PO_4, and 6 mM H_3PO_4 (10).

Dry weight. Biomass dry weight was measured in duplicate samples via filtration and drying as described previously for *P. chrysogenum* (23) and *S. cerevisiae* (6). For sampling from labeling experiments, filters with mycelia were dried for 24 h at 70°C.

Preparation of cell extracts. For the preparation of cell extracts of *S. cerevisiae* strains, culture samples were harvested by centrifugation, washed twice with 10 mM potassium phosphate buffer (pH 7.5) containing 2 mM EDTA, and stored at −20°C. Before cell breakage, the samples were thawed at room temperature, washed, and resuspended in 100 mM potassium phosphate buffer (pH 7.5) containing 2 mM $MgCl_2$ and 2 mM dithiothreitol. Extracts were prepared by sonication with 0.7-mm glass beads at 0°C for 2 min at 0.5-min intervals with an MSE sonicator (150-W output; 8-μm peak-to-peak amplitude). Unbroken cells and debris were removed by centrifugation at 4°C (20 min; 36,000 × *g*). The purified cell extract was used for enzyme assays.

Pyruvate and phenylpyruvate decarboxylase assays. Pyruvate decarboxylase activity was measured at 30°C, immediately after the preparation of cell extracts, using a Tecan GENios Pro set (Tecan, Giessen, The Netherlands). The assay mixture contained, in a total volume of 300 μl, 40 mM imidazole-HCI buffer (pH 6.5), 0.2 mM thiamine pyrophosphate, 0.15 mM NADH, 88 U · ml^{-1} alcohol dehydrogenase, 5 mM $MgCl_2$, and cell extract. The reaction, which was monitored as a decrease of absorbance at 340 nm, was started by the addition of 50 mM pyruvate. Reaction rates were linearly proportional to the added amount of cell extract. Measurements for the calculation of enzymatic kinetic properties, K_m and V_{max}, were performed under the same conditions as those for the pyruvate decarboxylase activity measurements, using substrate concentrations ranging from 0 to 75 mM. Phenylpyruvate decarboxylase activity was measured by monitoring the reduction of NAD^+ in the presence of excess aldehyde dehydrogenase from yeast using a Hitachi model 100-60 spectrophotometer at 340 nm (Hitachi, Tokyo, Japan). The reaction mixtures contained, in a total volume of 1 ml, 100 mM KH_2PO_4-K_2HPO_4 buffer, pH 7.0, 2 mM NAD^+, 5 mM $MgCl_2$, 15 mM pyrazole, 0.2 mM thiamine diphosphate, and 1.75 U of yeast aldehyde dehydrogenase from yeast (Sigma-Aldrich, Zwijndrecht, The Netherlands) (dissolved in 1 mM dithiothreitol). The reaction was started with the addition of 5 mM phenylpyruvate. Reaction rates were linearly proportional to the amount of cell extract added.

Protein determination. Protein concentrations in cell extracts were determined by the Lowry method (42). Bovine serum albumin (Sigma-Aldrich, Zwijndrecht, The Netherlands) was used as the standard.

Isotopically instationary model. The general isotopically instationary model for the simulation ^{13}C-labeling experiments, developed previously

(56), was used to estimate the network fluxes derived from [U-^{13}C]-labeled L-phenylalanine. Simulation and parameter estimation were carried out with a tool developed in Matlab (Mathworks, Natick, MA) and gPROMS (Process Systems Enterprise Limited, London, United Kingdom)

Transcriptome analysis. Chemostat culture broth (60 ml) was rapidly sampled and filtered over a glass fiber filter (type A/E; Pall Life Sciences, East Hills, NY). The filter containing the mycelium was immediately wrapped in aluminum foil, quenched in liquid nitrogen, and stored at −80°C. Samples were processed as described previously (26, 71). The acquisition and quantification of microarray images and data filtering were performed using Affymetrix GeneChip Operating Software (GCOS; version 1.2). Arrays were globally scaled to a target value of 100 using the average signals from all probe sets. The arrays were analyzed as previously described (26). Significant changes in the expression of the replicate arrays experiments were assessed statistically by using the software Significance Analysis of Microarrays (SAM; version 1.21) (70). The fold change (FC) was set to 2, and the false discovery rate was set to 1%.

Nucleotide sequence accession numbers. The coding sequences of Pc13g09300 and Pc18g01490 were deposited in GenBank under accession number JQ086348 and JQ086347, respectively. The sequence of the *pahA* gene from *P. chrysogenum* DS17690 has been deposited in GenBank under accession number JQ086346.

Microarray data accession numbers. Transcriptome data analyzed in this study have been deposited at the Genome Expression Omnibus database (http://www.ncbi.nlm.nih.gov/geo/) under accession number GSE32097.

RESULTS

Growth of *P. chrysogenum* on phenylalanine as a nitrogen source: penicillin G production in the absence of added phenylacetate acid. To investigate the capacity of *P. chrysogenum* DS17690 for the synthesis of penicillin G using either phenylacetate or phenylalanine, the strain was grown in glucose-limited chemostat cultures with phenylalanine as the nitrogen source. The normal startup process for a *P. chrysogenum* chemostat culture involves three phases: a batch phase, a fed-batch phase, and a chemostat phase (12). When phenylalanine was used as the nitrogen source, significant concentrations of phenylacetate and penicillin G were observed in all three phases of two independent replicate runs (Fig. 1). In reference experiments in which ammonium sulfate was added as the nitrogen source and phenylacetate was not included in the medium, concentrations of phenylacetate and penicillin G remained below their detection limits (0.01 and 0.02 mM, respectively). These results demonstrate that the side chain precursor phenylacetate can be formed from phenylalanine. In addition to phenylacetate and penicillin G, tyrosine and homogentisate were detected in culture supernatants of cultures grown with phenylalanine as the nitrogen source (Fig. 1).

During the continuous cultivation phase of the chemostat cultures, the biomass concentration stabilized at ca. 7 g · liter^{-1} (Fig. 1). The apparent biomass yield on glucose in the continuous cultivation phase was 0.92 ± 0.03 g biomass (g glucose)$^{-1}$, which is 2.5-fold higher than the biomass yield of chemostat cultures grown under the same conditions with ammonium sulfate as the nitrogen source (0.37 ± 0.00 g biomass [g glucose]$^{-1}$) (these data are from three independent steady-state chemostat cultures). This increase in biomass yield indicates that in addition to using phenylalanine as a nitrogen source, *P. chrysogenum* DS17690 is able to use this amino acid as a carbon and/or energy source. Consistent with this conclusion, extracellular concentrations of phenylalanine decreased to the analytical detection limit (50 μM), and free ammonia was detected in the continuous cultures at concentrations of ca. 2.5 mM (Fig. 1).

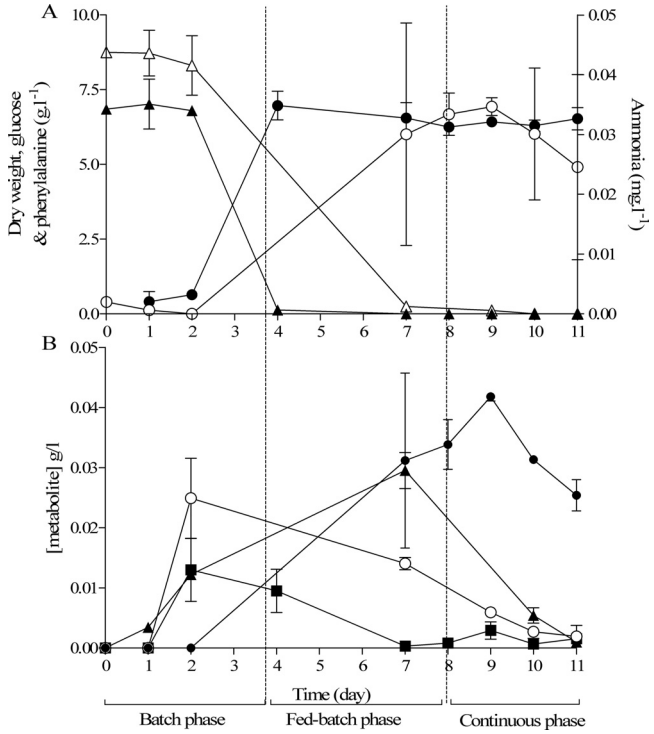

FIG 1 Biomass and extracellular metabolite profiles of *P. chrysogenum* DS17690 during batch cultivation, the fed-batch phase, and the continuous cultivation phase in two replicate glucose-limited chemostat experiments with phenylalanine as the nitrogen source (dilution rate, 0.05 h^{-1}; temperature, 25°C; pH 6.5). (A) Levels of biomass dry weight (closed circle) and concentrations of ammonia (open circle), glucose (closed triangle), and phenylalanine (open triangle) are expressed in g · liter^{-1}. (B) Concentrations of phenylacetate (open circle), homogentisate (closed square), tyrosine (closed triangle), and penicillin G (closed circle) are expressed in g · liter^{-1}. The time scale is expressed in days. Data are presented as averages ± mean deviations from independent duplicate cultures.

Although biomass concentrations (Fig. 1) and respiration rates (data not shown) stabilized during the continuous cultivation phase, extracellular concentrations of phenylalanine and other metabolites derived from aromatic amino acid metabolism continued to decrease during the continuous cultivation phase (Fig. 1). This precluded a precise comparison of penicillin G production rates to those observed in cultures to which the side chain precursor phenylacetate has been added. However, throughout the continuous cultivation phase, concentrations of penicillin G in the phenylalanine-grown cultures were about 20-fold lower than those in corresponding phenylacetate-supplemented cultures grown with ammonium sulfate as the nitrogen source (30 versus 600 mg · liter^{-1} of extracellular penicillin G). Combined with the 2.5-fold higher biomass concentration in the phenylalanine-grown cultures, this indicated that the biomass-specific rate of penicillin G in the latter cultures was about 2% of that in phenylacetate-supplemented cultures.

Quantitative analysis of phenylalanine flux distribution in *Penicillium chrysogenum*. To determine the *in vivo* flux distribution of phenylalanine in *P. chrysogenum*, glucose-limited chemostats with unlabeled phenylalanine were first grown to steady state,

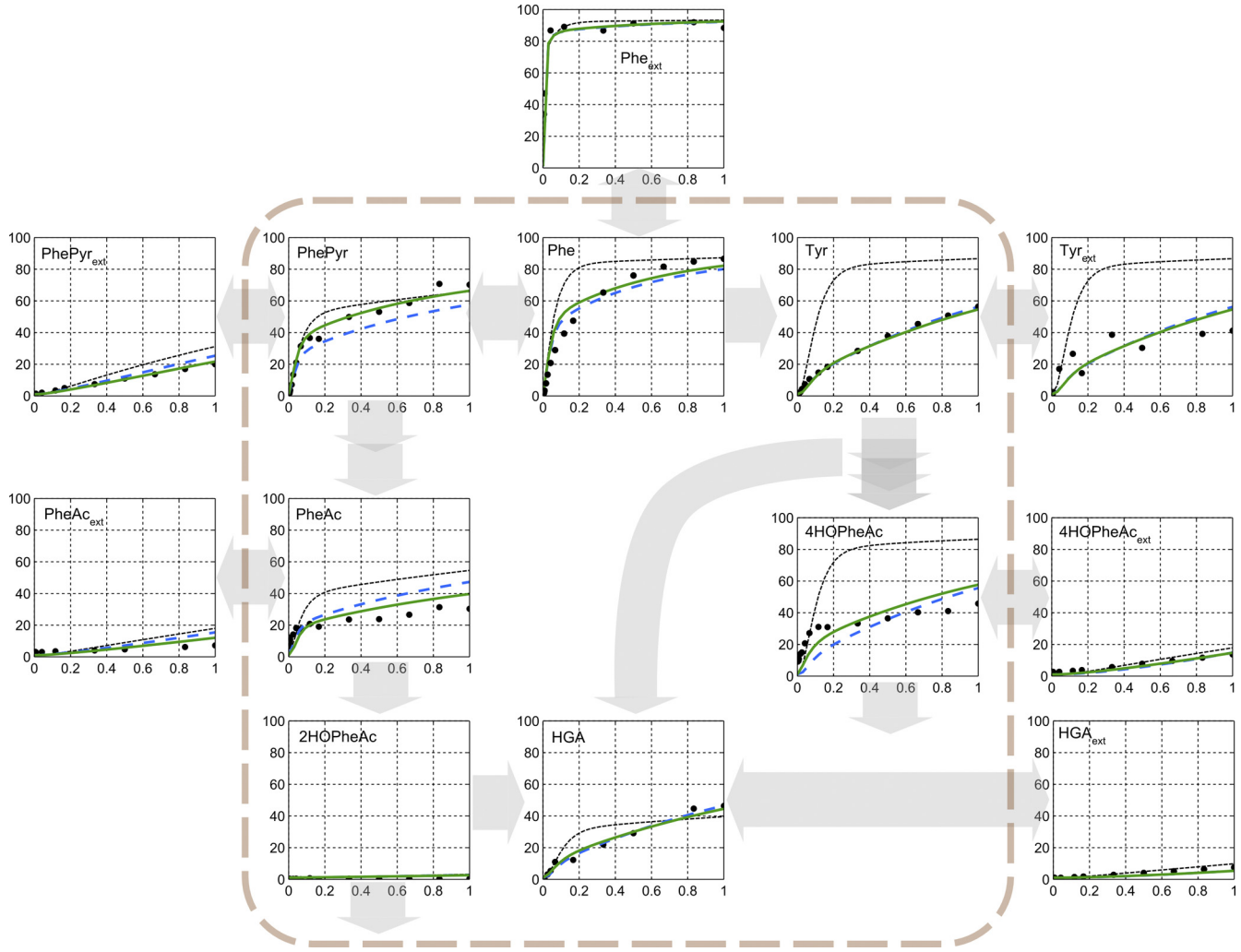

FIG 2 Measured and calculated ^{13}C enrichment of intra- and extracellular metabolite profiles obtained after switching a *P. chrysogenum* DS17690 glucose-limited chemostat culture (dilution rate, 0.05 h^{-1}; temperature, 25°C; pH = 6.5) grown with L-phenylalanine as the sole nitrogen source to a medium containing [U-^{13}C]-labeled phenylalanine. The *x* axes of the graphs represent the sampling period expressed in hours. The lines indicate three modeling scenarios (see Results). Scenario i is presented with black dashed lines, scenario ii is represented with blue dashed-dotted lines, and scenario iii is represented with green lines. A full description of the reaction networks for the different scenarios is provided in Table S3 in the supplemental material. Phe, phenylalanine; Phe$_{ext}$, extracellular phenylalanine; Tyr, tyrosine; Tyr$_{ext}$, extracellular tyrosine; PhePyr, phenylpyruvate; PhePyr$_{ext}$, extracellular phenylapyruvate; PheAc, phenylacetate; PheAc$_{ext}$, extra cellular phenylacetate; 4HOPheAc, 4-hydroxyphenylacetate; 4HOPheAc$_{ext}$, extracellular 4-hydroxyphenylacetate; 2HOPheAc, 2-hydroxyphenylacetate; HGA, homogentisate; HGA$_{ext}$, extracellular homogentisate.

based on biomass concentration and the CO_2 biomass-specific production rate on unlabeled substrate, and then switched to a medium that contained [U-^{13}C]-labeled L-phenylalanine. Samples for intracellular and extracellular metabolite concentration measurements were taken before and after the switch to the labeled substrate, and then enrichment was measured during a period of 1 h.

In the [U-^{13}C]L-phenylalanine feeding experiments, only a small fraction of the phenylalanine was recovered as penicillin G. The measured uptake rate of L-phenylalanine was 307 $\mu mol^{-1} \cdot (g\ dry\ biomass)^{-1} \cdot h^{-1}$, and the penicillin G production rate was below 1 $\mu mol^{-1} \cdot (g\ dry\ biomass)^{-1} \cdot h^{-1}$. The extracellular accumulation of fully labeled phenylpyruvate, phenylacetate, tyrosine, 4-hydroxyphenylacetate, 2-hydroxyphenylacetate, and homogentisate (Fig. 2 and Table 2) confirmed the *in vivo* activity of a phenylalanine hydroxylase in *P. chrysogenum* as well as of a homogentisate pathway for phenylalanine catabolism (Table 2 and Fig. 2). The overall activity of the 2-hydroxyphenylacetate pool was 10-fold lower than that of phenylacetate, which is consistent with two previously reported single-nucleotide mutations ($598^{C\rightarrow T}$, $1357^{C\rightarrow T}$) in the phenylacetate hydroxylase gene (*pahA*) that lead to a near-complete elimination of enzyme activity (61). The presence of these mutations in *P. chrysogenum* DS17690 was confirmed by the resequencing of *pahA* (data not shown).

An immediate enrichment of intracellular metabolites with ^{13}C-labeled carbon atoms was observed upon the switch to the labeled L-phenylalanine (Fig. 2). Intracellular L-phenylalanine reached an enrichment of 50% after about 10 min, which was significantly slower than the dynamics of the extracellular pool (50% after 30 s). Phenylpyruvate reached 50% enrichment after about 20 min and tyrosine after 50 min. The remaining metabolites did not reach 50% enrichment within 1 h. For the quantita-

TABLE 2 Extra- and intracellular metabolite concentrations of phenylalanine catabolism pathway in *P. chrysogenum*[a]

Metabolite	Metabolite concn			IC/EC concn ratio
	EC (μmol · liter^{-1})	IC (μmol · [g dry wt]$^{-1}$)	IC (μmol · [liter^{-1}])	
Phenylacetate	79	0.1	35	0.4
2-Hydroxy phenylacetate	7	0	3	0.4
L-Phenylalanine	24	20	7919	324
Phenylpyruvate	939	0.3	110	0.1
Homogentisate	339	ND	ND	

[a] *P. chrysogenum* DS17690 was grown in glucose-limited chemostat cultures with phenylalanine as the sole nitrogen source. A cellular volume of 2.5 ml · (g dry weight)$^{-1}$ was assumed (58). EC, extracellular; IC, intracellular. ND, not detected.

tive evaluation of the enriched fractions, a metabolic reaction network was constructed and the respective C-atom transitions were calculated (see Table S3 in the supplemental material). To evaluate the different hypotheses, the distribution of three scenarios was considered (Table 3).

In the first model, the concurrent linear reactions were included; a reaction network was used in which phenylalanine was either incorporated into protein, incorporated into penicillin G, metabolized via the homogentisate pathway, or metabolized via tyrosine (scenario i) (see Table S3 in the supplemental material). Stoichiometric coefficients for tyrosine and phenylalanine incorporation into *P. chrysogenum* protein were taken from reference 72 (Table 2). Scenario i reproduced the observed enrichment profile of extracellular L-phenylalanine and, to a certain extent, phenylpyruvate. However, dynamics of other metabolites could not be reproduced. The enrichment prediction rates were much faster than the measured values (Table 3 and Fig. 2).

In scenario ii, an additional hypothetical pathway for phenylalanine metabolism, which did not involve any of the measured metabolites, was introduced into the model (flux for phenylalanine degradation in Table S3 in the supplemental material), as well as an exchange of phenylalanine and tyrosine with the protein pool (synthesis and degradation). This led to a significant (60%) diversion of the predicted labeled inflow of phenylalanine into the unknown sink, which reduced predicted fluxes into the homogentisate and tyrosine branches compared to those of scenario i and strongly improved the reproduction of the experimental data (Table 3 and Fig. 2). This observation indicates that in addition to metabolism via the tyrosine and homogentisate pathways, *P. chrysogenum* contains additional pathways for phenylalanine utilization.

A model based on scenario ii still did not correctly reproduce the dynamics of phenylpyruvate, phenylacetate, and 4-hydroxyphenylacetate (Fig. 2). In particular, the calculated ^{13}C enrichments in the later phase of the experiments (>30 min) were too high for phenylacetate and too low for phenylpyruvate. Therefore, in scenario iii (Table 3; also see Table S3 in the supplemental material), hypothetical hydroxylase activities were included that convert phenylpyruvate to 4-hydroxyphenylpyruvate and phenylacetaldehyde to 4-hydroxyphenylacetaldehyde, thereby effectively connecting the two pathways of phenylalanine catabolism (Fig. 3 and Table 3; also see Table S3).

With the reaction network based on scenario iii, the model predictions for the enrichment of phenylpyruvate, phenylacetate, tyrosine, and homogentisate closely resembled the experimental observations. Compared to those of scenario ii, in scenario iii the flux from L-phenylalanine to phenylpyruvate was increased, while the flux to phenylacetate was reduced by branching into 4-hydroxyphenylacetate (Table 3). Around 14% of the L-phenylalanine was directed via these two reactions.

Transcriptome analysis of phenylalanine and ammonium sulfate-grown *P. chrysogenum*. To gain more insight into possible pathways for phenylalanine metabolism in *P. chrysogenum*, the transcriptomes of aerobic glucose-limited chemostat cultures of *P. chrysogenum* grown with either phenylalanine or ammonium sulfate as the nitrogen source were analyzed using DNA microarrays. The average coefficient of variation for biological replicates (triplicates for the carbon-limited cultures with ammonium sul-

TABLE 3 Intracellular net fluxes obtained by growing *P. chrysogenum* with medium containing [U-^{13}C]-labeled phenylalanine

Reaction	Intracellular net flux (μmol · [g dry weight]$^{-1}$ · h^{-1}) for scenario[a]:		
	i (initial model)	ii (with protein exchange)	iii (with protein exchange and hydroxylase)
Phenylalanine uptake	306.7	306.7	306.7
Penicillin G production	12.2	13.3	3.5
Phenylalanine→phenylpyruvate	18.1	19.3	51.5
Phenylalanine→tyrosine	280.2	85.6	63.8
Phenylalanine→unknown sink	0.0	193.5	183.1
Phenylalanine→4-hydroxyphenylpyruvate	0.0	0.0	21.6
Phenylacetaldehyde→4-hydroxyphenylacetaldehyde	0.0	0.0	20.4

[a] Three different network scenario hypotheses were employed to obtain an optimal fit for flux distribution: scenario i, phenylalanine was incorporated into protein, incorporated into penicillin G, metabolized via the homogentisate pathway, or metabolized via tyrosine; scenario ii, an unidentified pathway for phenylalanine metabolism, which did not involve any of the measured metabolites, was introduced into the model together with exchanges of phenylalanine and tyrosine with the protein pool (synthesis and degradation); and scenario iii, hypothetical hydroxylase activities that convert phenylpyruvate to 4-hydroxyphenylpyruvate and phenylacetaldehyde to 4-hydroxyphenylacetaldehyde were included.

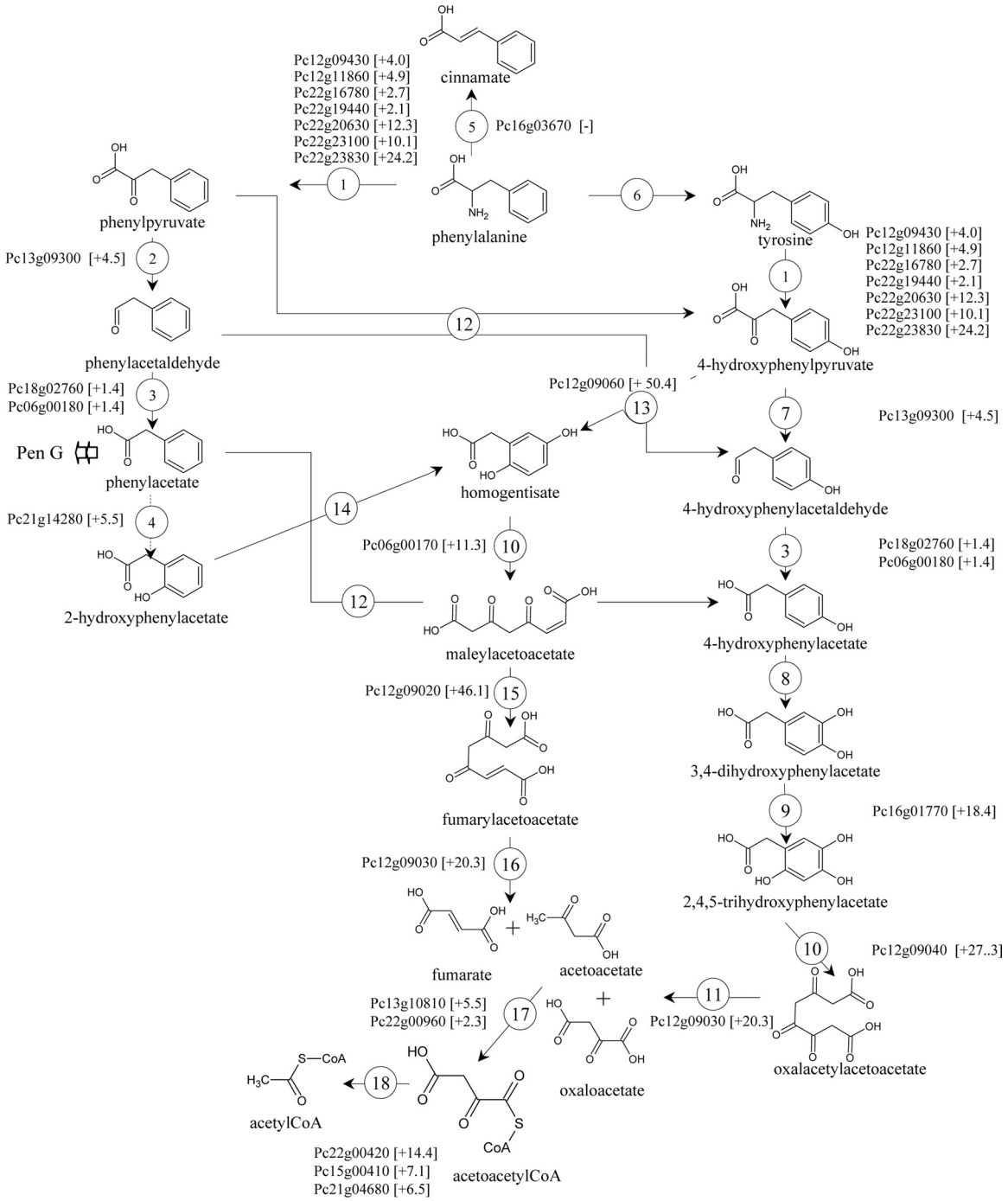

FIG 3 Pathways for L-phenylalanine metabolism in *P. chrysogenum*. Shown are genes that are possibly involved in phenylalanine metabolism and that were found to be upregulated in cultures with phenylalanine as the nitrogen source. The values between brackets represent the average fold changes in the expression of phenylalanine-grown cultures relative to levels of expression in ammonium-grown cultures. 1, aromatic amino acid transaminase; 2, phenylpyruvate decarboxylase; 3, aldehyde dehydrogenase; 4, phenylacetate hydroxylase; 5, phenylalanine ammonia lyase; 6, phenylalanine hydroxylase; 7, 4-hydroxyphenylacetate decarboxylase; 8, 4-hydroxyphenylacetate 3-hydroxylase; 9, 3-hydroxyphenylacetate 6-hydroxylase; 10, homogentisate dioxygenase; 11, oxalacetylacetoacetate hydrolase; 12, putative hydroxylase; 13, 4-hydroxyphenylacetate dioxygenase; 14, 2-hydroxyphenylacetate 5-hydroxylase; 15, maleylacetoacetate isomerase; 16, fumarylacetoacetate hydrolase; 17, acetoacetyl-CoA synthase; 18, acetyl-CoA acetyltransferase.

fate and duplicates for the carbon-limited cultures with phenylalanine) were below 20%. This value is in accordance with values generally obtained from previous chemostat-based genome-wide expression monitored in *P. chrysogenum* (14, 26, 27, 36, 68, 71).

The pairwise comparison of phenylalanine- to ammonium sulfate-grown cultures yielded a total of 331 genes that were differentially expressed ($|FC| > 2$; false discovery rate of 0.01%). Of these 331 genes, 291 were expressed at a higher level in the phe-

TABLE 4 MIPS functional categories overrepresented in the selected set of genes[c]

MIPS category	Description	*k*[a]	*n*[b]	*P* value
Significantly ($P < 1.0E-03$) overrepresented in upregulated genes ($n = 291$)				
01	Metabolism	137	2472	3.52E−29
01.01	Amino acid metabolism	55	467	2.3E−25
01.01.01	Amino acid biosynthesis	17	205	2.4E−06
01.01.01.15	Biosynthesis of the pyruvate family (Ala, Ile, Leu, Val)	5	26	2.1E−04
01.01.10	Amino acid degradation (catabolism)	34	170	2.2E−23
01.01.10.01	Degradation of amino acids of the glutamate group	8	28	9.7E−08
01.01.10.01.01	Degradation of proline	3	10	1.1E−03
01.01.10.01.04	Degradation of glutamate	5	9	5.5E−07
01.01.10.04	Degradation of amino acids of the pyruvate family	9	19	7.4E−11
01.01.10.04.02	Degradation of valine	4	12	9.5E−05
01.01.10.04.03	Degradation of leucine	6	13	1.5E−07
01.01.10.04.04	Degradation of isoleucine	3	8	5.3E−04
01.01.10.05	Degradation of amino acids of the cysteine-aromatic group	12	62	7.3E−09
01.01.10.05.05	Degradation of phenylalanine	6	30	3.9E−05
01.01.10.05.06	Degradation of tyrosine	6	15	4.3E−07
01.05	C compound and carbohydrate metabolism	49	1069	4.5E−07
01.05.01	C compound and carbohydrate utilization	46	760	2.3E−10
01.05.01.01	C compound, carbohydrate catabolism	18	377	2.3E−04
01.05.01.01.03	C_2 compound and organic acid catabolism	6	29	3.1E−05
01.06	Lipid, fatty-acid and isoprenoid metabolism	31	410	1.5E−09
01.06.01	Lipid, fatty-acid and isoprenoid biosynthesis	17	252	3.8E−05
01.06.04	Breakdown of lipids, fatty acids and isoprenoids	9	91	1.6E−04
01.06.07	Lipid, fatty-acid and isoprenoid utilization	7	52	1.2E−04
01.20.15	Biosynthesis of derivatives of dehydroquinate, shikimate and chorismate	3	10	1.1E−03
02	Energy	26	312	4.6E−09
02.16	Fermentation	5	36	1.0E−03
02.25	Oxidation of fatty acids	4	13	1.3E−04
40	Subcellular localization	88	2434	3.4E−07
40.03	Cytoplasm	25	577	8.3E−04
40.16	Mitochondrion	33	348	9.7E−13
40.19	Peroxisome	8	68	1.1E−04
67.04.01.01.01	Siderophore-iron transporter	4	16	3.2E−04
Significantly ($P < 1.0E-03$) overrepresented in downregulated genes ($n = 40$)				
01.06	Lipid, fatty-acid and isoprenoid metabolism	8	410	1.9E−05
01.06.01	Lipid, fatty-acid and isoprenoid biosynthesis	6	252	8.1E−05
01.06.01.07	Isoprenoid biosynthesis	4	104	2.3E−04
01.06.01.07.07	Diterpene biosynthesis	2	11	4.4E−04
01.06.99	Other lipid, fatty-acid and isoprenoid metabolism activities	2	15	8.4E−04
11	Cell rescue, defense and virulence	9	809	4.2E−04
11.07	Detoxification	6	379	7.3E−04

[a] *k* represents the number of genes in the MIPS category found to be differentially expressed.
[b] *n* represents the number of genes of the same MIPS category found in the whole genome.
[c] Shown are MIPS functional categories overrepresented in the set of genes significantly differentially expressed (|FC| > 2; false discovery rate, 1%) in glucose-limited chemostat cultures of *P. chrysogenum* grown with phenylalanine as the nitrogen source relative to results for cultures grown with ammonium sulfate as the nitrogen source. *P* values were calculated via Fischer exact statistics.

nylalanine cultures, and 40 exhibited the inverse profile (see Table S4 in the supplemental material). These two groups of genes were analyzed for the overrepresentation of functional categories using Fischer's exact test.

Genes involved in amino acid degradation were clearly overrepresented in the set of 291 genes that showed an increased transcript level when phenylalanine was used as the nitrogen source. This overrepresentation was found not only for genes involved in the degradation of aromatic amino acids but also for genes involved in the degradation of branched-chain amino acids and glutamate-, proline-, and sulfur-containing amino acids (Table 4). Among the same set of 291 genes, a significant subset of 46 transcripts (16%; $P > 1.0E-04$) were previously shown to exhibit an increased transcript level in chemostat cultures supplemented with phenylacetate (see Table S5 in the supplemental material) (26). This subset comprised genes that, based on sequence homology, are expected to encode enzymes involved in the homogentisate pathway, e.g., phenylacetate hydroxylase (Pc21g14280 and *pahA*), maleylacetoacetate isomerase (Pc12g09020), fumarylacetoacetase (Pc12g09030), acetoacetyl-coenzyme A (CoA) synthase (Pc22g00960), 3,4-dihydroxyphenylacetate-2,3-dioxygenase (Pc12g09040), and a transcription factor similar to *S. cerevisiae* Aro80 (Pc12g09010). In contrast,

the putative homogentisate pathway genes encoding 4-hydroxyphenylpyruvate dioxygenase (Pc12g09060) and gentisate-1,2-dioxygenase (Pc06g00170), which convert 4-hydroxyphenylpyruvate to homogentisate and homogentisate to maleylacetoacetate, were upregulated in phenylalanine-grown cultures but not in cultures supplemented with phenylacetate (Fig. 3). These transcriptional modifications confirm the involvement of the homogentisate pathway in phenylalanine catabolism by *P. chrysogenum*.

P. chrysogenum DS17690 exhibits extremely low conversion of phenylacetate to 2-hydroxyphenylacetate, which is consistent with the $598^{C\rightarrow T}$ mutation in its *pahA* gene (61). Labeling experiments indicated the activity of an alternative route toward homogentisate, starting with the hydroxylation of phenylalanine to tyrosine. Several uncharacterized hydroxylases were strongly upregulated in cultures grown with phenylalanine as the nitrogen source (Pc06g01260, Pc16g01770, Pc13g01500, Pc13g05260, Pc20g02710, Pc22g11860, Pc22g18500, Pc22g23500, and Pc22g24900). However, sequence analysis did not reveal a significant similarity of any of these genes to known eukaryotic or prokaryotic phenylalanine hydroxylases. Interestingly, although it has already been proposed to be present in *A. nidulans* but has never been demonstrated (17, 18), phenylalanine hydroxylase has not been detected in *A. niger* (35), and no fungal phenylalanine hydroxylase genes have been cloned yet.

The measurement of [^{13}C]phenylpyruvate and [^{13}C]phenylacetate confirmed the occurrence of a metabolic route similar to that of the Ehrlich pathway in *S. cerevisiae* (28). The first and third steps in this pathway are the transamination of phenylalanine to phenylpyruvate and the oxidation of phenylaldehyde to phenylacetate, respectively (Fig. 3). Seven genes (Pc12g09430, Pc12g11860, Pc22g16780, Pc22g19440, Pc22g20630, Pc22g23100, and Pc22g23830) with high similarity to known transaminases were significantly upregulated in phenylalanine-grown cultures. Interestingly, Pc12g11860 exhibited more than 50% sequence similarity (E value $<$ 6E$-$129) to *S. cerevisiae ARO8*, which encodes one of the two aromatic amino acid aminotransferases. No gene encoding an aldehyde dehydrogenase was differentially expressed. Out of the 9 putative aldehyde dehydrogenase genes identified in *P. chrysogenum* (Pc14g01080, Pc21g22810, Pc22g24860, Pc18g02760, Pc14g01040, Pc22g17230, Pc20g11160, Pc22g19300, and Pc06g00180), only three were expressed in at least one condition. Pc21g22810 was expressed only on ammonia cultures, disqualifying it for actively participating in this pathway. The two remaining genes, Pc18g02760 and Pc06g00180, exhibited a slight upregulation on phenylalanine with a fold change of +1.4 each. However, Pc06g00180 might be the most prominent one, as its expression level was 16-fold higher than that of Pc18g02760. Finally, we focused on the second step of the Ehrlich pathway, in which phenylpyruvate is decarboxylated to phenylacetaldehyde (Fig. 3). In *S. cerevisiae*, *ARO10* encodes the main phenylpyruvate decarboxylase (74, 75). A search for *ARO10* homologs in the *P. chrysogenum* genome sequence (comprising 13,670 proteins; GenBank accession numbers AM920416 to AM920464) (71), using the Aro10p amino acid sequence as a query, revealed three open reading frames with a sequence similarity above 50% (E value $<$ 6E$-$50): Pc18g01490, Pc13g09300, and Pc16g13320. Whereas Pc16g13320 was not expressed under the conditions tested in this study, Pc18g01490 and Pc13g09300 were strongly upregulated in cultures grown with phenylalanine (fold changes of 12.8 and 4.3, respectively). To investigate whether these genes indeed encode fungal 2-oxo acid decarboxylases involved in the production of phenylacetate via an Ehrlich-type pathway (Fig. 3), they were functionally characterized via their expression in *S. cerevisiae*.

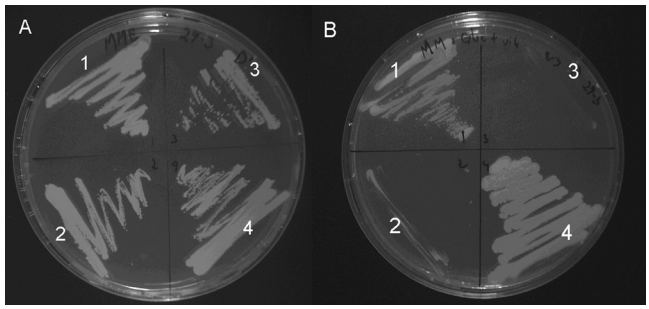

FIG 4 Growth of two *S. cerevisiae* strains expressing putative *P. chrysogenum* 2-oxo acid decarboxylase genes and their controls, a thiamine pyrophosphate-dependent 2-oxo acid decarboxylase-free strain and its positive control, on synthetic medium agar plates with ethanol (A) and glucose (B). Ethanol plates were incubated for 7 days, and glucose plates were incubated for 3 days at 30°C. Strain 1, IMZ245 (*pdc1*Δ *pdc5*Δ *pdc6*Δ *aro10*Δ *thi3*Δ Pc13g09300); strain 2, IMZ246 (*pdc1*Δ *pdc5*Δ *pdc6*Δ *aro10*Δ *thi3*Δ Pc18g01490); strain 3, IMZ001 (*pdc1*Δ *pdc5*Δ *pdc6*Δ *aro10*Δ *thi3*Δ); strain 4, IME004 (*PDC1 PDC5 PDC6 ARO10 THI3*).

Expression of Pc13g09300 in *S. cerevisiae*: evidence for a pyruvate and phenylpyruvate decarboxylase gene in *P. chrysogenum*. *S. cerevisiae* contains five homologous open reading frames that have been implicated in the synthesis of 2-oxo acid decarboxylases. *PDC1*, *PDC5*, and *PDC6* encode pyruvate decarboxylase isozymes (30, 31), *ARO10* codes for a phenylpyruvate decarboxylase with a broad substrate specificity (75), and *THI3* codes for a putative decarboxylase (28). A strain deleted for the five decarboxylase genes cannot grow on glucose in batch cultures, because in *S. cerevisiae* pyruvate decarboxylase activity is an essential enzyme for growth on glucose (21). Moreover, since an active Ehrlich pathway is required for growth on phenylalanine as the nitrogen source, it also cannot grow on phenylalanine as the sole nitrogen source (74). The strain *S. cerevisiae* CEN-PK711-7C, which bears these quintuple deletions, was transformed with plasmids carrying overexpression cassettes for the putative decarboxylase genes Pc18g01490 and Pc13g09300, resulting in strains IMZ245 (Pc18g01490) and IMZ246 (Pc13g09300). The two overexpression strains were grown on synthetic medium agar plates with 2% glucose as the sole carbon source along with control strains IMZ001 (quintuple-deletion CEN.PK711-7C transformed with the empty plasmid p426GPD) and the positive control IME004 (*PDC1 PDC5 PDC6 THI3 ARO10*).

Only *S. cerevisiae* IMZ245 (Pc13g09300) and the positive control (IME044) were able to grow on glucose (Fig. 4). Consistently with a pyruvate decarboxylase activity of Pc13g09300, ethanol was formed in glucose-grown shake flask cultures of IMZ245 (synthetic medium with 2% glucose; data not shown). Neither IMZ001 nor IMZ246 grew in shake flask culture with glucose as the sole carbon source, confirming the plate assay results. These data demonstrate that Pc13g09300, but not Pc18g01490, encodes a pyruvate decarboxylase. To test the ability of the two decarboxylases to restore the growth of the quintuple deletion strain on phenylalanine as the sole nitrogen source, *S. cerevisiae* IMZ245 (Pc13g09300) was grown in an aerobic glucose-limited chemostat (dilution rate, 0.05 h^{-1}) with phenylalanine as a nitrogen source.

TABLE 5 Specific pyruvate and phenylpyruvate decarboxylase activities in cell extracts of *S. cerevisiae* IMZ245 (Pc13g09300)[a]

Nitrogen source	Sp act (nmol · [mg protein]$^{-1}$ · min^{-1}) of:	
	Pyruvate decarboxylase	Phenylpyruvate decarboxylase
$(NH_4)_2SO_4$	287 ± 9	11 ± 2
Phenylalanine	314 ± 41	17 ± 2

[a] *S. cerevisiae* IMZ245 (Pc13g09300) was grown in aerobic glucose-limited chemostat cultures, with $(NH_4)_2SO_4$ or phenylalanine as the nitrogen source, at a dilution rate of 0.05 h^{-1}. Data are presented as averages ± mean deviations from independent duplicate measurements.

S. cerevisiae IMZ246 was grown under the same conditions but with ethanol instead of glucose as the carbon source to investigate the possibility that Pc18g01490 encodes a specific phenylpyruvate decarboxylase. Only strain IMZ245 (Pc13g09300) was able to grow on phenylalanine, with a biomass yield of 0.29 g · (g glucose)$^{-1}$ and a biomass-specific phenylacetate production rate of 0.156 mmol · (g biomass)$^{-1}$ · h^{-1}. These data indicate that Pc13g09300 encodes a pyruvate decarboxylase that also can decarboxylate phenylpyruvate.

Characterization of the (phenyl)pyruvate decarboxylase encoded by Pc13g09300. To further characterize the decarboxylase encoded by Pc13g09300, cell extracts prepared from aerobic, glucose-limited chemostat cultures of *S. cerevisiae* IMZ245 were grown with either phenylalanine or $(NH_4)_2SO_4$ as the nitrogen source. Enzyme activity assays revealed a clear pyruvate decarboxylase activity in the extracts of both phenylalanine- and $(NH_4)_2SO_4$-grown cultures. A 15-fold lower phenylpyruvate decarboxylase activity was measured as well (Table 5). In contrast to Aro10p in *S. cerevisiae*, which has much higher activity in cultures grown with phenylalanine as the nitrogen source than in cultures grown with ammonium sulfate as the nitrogen source (74) due to a posttranscriptional regulation process, no drastic effect of the nitrogen source on the activity of Pc13g09300 was observed. The phenylpyruvate decarboxylase activity measured in cell extracts of glucose-limited chemostat cultures grown with phenylalanine as the nitrogen source (17 nmol · [mg protein]$^{-1}$ · min^{-1}) was sufficient to explain the *in vivo* flux toward phenylacetate (8 nmol · [mg protein]$^{-1}$ · min^{-1}), which was calculated from data shown in Table 3 based on a soluble protein content of yeast biomass of 33% (60).

When pyruvate decarboxylase activities were assayed at pyruvate concentrations ranging from 0 to 75 mM, a sigmoidal relationship between substrate concentration and reaction rate was observed that could be fitted with the Hill equation (29). The estimated kinetic properties of Pc13g09300 in cell extracts were $K_m = 13.8$ mM and $V_{max} = 2.1$ μmol (mg protein)$^{-1}$ · min^{-1} with pyruvate as the substrate. The derived Hill coefficient of 2.0 indicated that, similarly to pyruvate decarboxylases from other organisms (7, 32), this fungal pyruvate decarboxylase exhibits cooperativity with respect to pyruvate.

DISCUSSION

Phenylalanine utilization in *P. chrysogenum*. Since the 1940s, the industrial production of penicillin G fermentations has relied on the addition of phenylacetate to fermentation media. This study shows that both phenylacetate and penicillin G can be produced *in vivo* from the catabolism of phenylalanine via an Ehrlich-type pathway that involves phenylpyruvate decarboxylation as a key reaction. Although fluxes from phenylalanine toward phenylacetate and penicillin G were low, they provide an adequate explanation for the beneficial effect of complex medium components, such as corn steep liquor, on penicillin G production in early studies (50–52).

The model-based analysis of ^{13}C-labeled metabolite pools suggests the involvement of an Ehrlich-type pathway involving subsequent transamination, decarboxylation, and oxidation reactions, combined with draining reactions catalyzed by hydroxylases that act upon the intermediates of this pathway. The metabolic branch toward phenylpyruvate and onward resembles metabolism already described for several fungal species (35, 47–49). Furthermore, the modeling results suggest the conversion of phenylalanine to tyrosine via a phenylalanine hydroxylase.

The cinnamate pathway, which is involved in phenylalanine catabolism in several ascomycetes (e.g., *Aspergillus oryzae*) and basidiomycetes (33, 65), is unlikely to contribute to phenylalanine catabolism under the conditions employed in the present study. No labeled cinnamate was detected in intra- and extracellular metabolite samples from phenylalanine-grown *P. chrysogenum* cultures, and moreover, Pc16g03670, the *P. chrysogenum* ortholog of the *A. oryzae* phenylalanine ammonia lyase (XP_001826366.2), was not expressed when phenylalanine was added as the nitrogen source or when ammonium sulfate fulfilled this role.

Testing the hypothesis that phenylalanine hydroxylase contributes to phenylalanine catabolism in *P. chrysogenum*, which is in contrast to the assumption that this pathway is absent from ascomycetous fungi, will require an in-depth functional analysis of putative hydroxylase genes in this fungus.

(Phenyl)pyruvate decarboxylase in *P. chrysogenum*. The presence of a 2-oxo acid decarboxylase in *P. chrysogenum* confirms that phenylacetate originates from a fungal Ehrlich-like pathway for phenylalanine catabolism, a conclusion that is further supported by the concerted transcriptional upregulation of Pc13g09300 and genes involved in the homogentisate pathway (Fig. 3). Pyruvate decarboxylases are broadly distributed in fungi and plants, and scientific interest is related mainly to their crucial role in alcoholic fermentation. The role of pyruvate decarboxylases in aerobic, nonfermentative organisms such as *P. chrysogenum* is incompletely understood. Several examples suggest that alcoholic fermentation contributes to the short-term anaerobic survival of aerobic organisms (34, 41). For example, the deletion of the alcohol dehydrogenase gene *adhC* in *A. nidulans* reduces the ability of this fungus to survive long periods of anaerobic stress. This could be an explanation for the fact that *A. nidulans* does not appear to have other pathways for regenerating NAD^+ in the absence of oxygen (34). In *Rhizopus oryzae*, the expression of the genes encoding the two pyruvate decarboxylases, *pdcA* and *pdcB*, is tightly connected to hypoxic stress and was correlated with the formation of ethanol (67). Our work demonstrates the existence of a functional pyruvate decarboxylase in *P. chrysogenum*. The high expression of Pc13g09300 in aerobic cultures grown with phenylalanine as the nitrogen source indicates that the transcriptional regulation of pyruvate decarboxylase is not exclusively related to anaerobicity. The demonstration that, in addition to its pyruvate decarboxylase activity, Pc13g09300 utilizes phenylpyruvate as a substrate raises the possibility that this and other fungal pyruvate decarboxylase genes are not subject to a dual regulation by oxygen status and nitrogen source. Moreover, by analogy to the situation in *S. cerevisiae* (28), it seems probable that Pc13g09300

and/or its two homologs in the *P. chrysogenum* genome are involved in Ehrlich-type pathways for the catabolism of other amino acids.

Metabolic engineering of phenylacetate supply in *P. chrysogenum*. In current industrial processes for the production of penicillin G with *P. chrysogenum*, phenylacetate has to be fed at a controlled rate to ensure that its concentration does not limit penicillin G synthesis while at the same time avoiding toxic side effects (77). The high costs derived from the external addition of phenylacetate, which is produced from petrochemistry, already has stimulated research into a more efficient use of phenylacetate (39, 61). The increased understanding of the native *P. chrysogenum* pathway for phenylalanine production, combined with the increased accessibility of this fungus to genetic modification (68), now make metabolic engineering strategies for the complete synthesis of penicillin G from glucose, ammonia, and sulfate a realistic prospect. A first objective in such metabolic engineering studies should be to increase the intracellular concentration of phenylacetate. This concentration would have to be optimized by increasing the flux through the phenylalanine biosynthetic pathway. To do so, strategies have already been applied in other organisms (i.e., *Escherichia coli* [43] and *S. cerevisiae* [44]). In *S. cerevisiae*, the simultaneous replacement of the 3-deoxy-D-arabino-heptulosonate-7-phosphate synthase (*ARO4*) and the chorismate mutase (*ARO7*) with tyrosine feedback-insensitive alleles ($ARO4^{K229L}$ and $ARO7^{G141S}$) led to a 4.5-fold increase of the *in vivo* flux toward phenylalanine (44). Subsequently, the synthesis of undesirable byproducts and the degradation of intermediates will have to be minimized. The identification and deletion of the gene(s) encoding putative phenylalanine and phenylpyruvate hydroxylase activities may be an essential requirement to fulfill this objective. The deletion of these genes in combination with the loss-of-function mutation in the phenylacetate hydroxylase (*pahA*) (61) gene might lead to an increased flux toward phenylacetate. Finally, the flux through phenylpyruvate decarboxylase should be improved by, for example, the replacement of the newly identified phenylpyruvate decarboxylase (Pc13g09300) with a heterologous enzyme with better kinetic properties. An interesting option is provided by the *S. cerevisiae* gene *ARO10*, which encodes a well-characterized phenylpyruvate decarboxylase (74, 75). In comparable experimental setups, Aro10p exhibited an *in vitro* phenylpyruvate activity that is 15-fold higher than the one found in this study for Pc13g09300 (270 nmol · [mg protein]$^{-1}$ · min^{-1} versus 16.7 nmol · [mg protein]$^{-1}$ min^{-1}). In addition to improved process economics, the replacement of petrochemically produced phenylacetate with a renewable sugar substrate can further improve the sustainability of large-scale penicillin G production.

ACKNOWLEDGMENTS

We acknowledge financial support from the Netherlands Organization for Scientific Research (NWO) via the IBOS (Integration of Biosynthesis and Organic Synthesis) Programme of Advanced Chemical Technologies for Sustainability (ACTS) (project no. IBOS 053.63.011).

We thank Remon Boer and Roel A. L. Bovenberg (from DSM) for their support during this project.

REFERENCES

1. **Alberti S, Gitler AD, Lindquist S.** 2007. A suite of Gateway cloning vectors for high-throughput genetic analysis in *Saccharomyces cerevisiae*. Yeast **24**:913–919.
2. **Arias-Barrau E, et al.** 2004. The homogentisate pathway: a central catabolic pathway involved in the degradation of L-phenylalanine, L-tyrosine, and 3-hydroxyphenylacetate in *Pseudomonas putida*. J. Bacteriol. **186**: 5062–5077.
3. **Backus MP, Stauffer JF.** 1955. The production and selection of a family of strains in *Penicillium chrysogenum*. Mycologia **47**:429–463.
4. **Behrens OK, Corse J.** 1948. Biosynthesis of penicillins; utilization of deuterophenylacetyl-N15-dl-valine in penicillin biosynthesis. J. Biol. Chem. **175**:765–769.
5. **Behrens OK, et al.** 1948. Biosynthesis of penicillins; biological precursors for benzylpenicillin (penicillin G). J. Biol. Chem. **175**:751–764.
6. **Boer VM, et al.** 2007. Transcriptional responses of *Saccharomyces cerevisiae* to preferred and nonpreferred nitrogen sources in glucose-limited chemostat cultures. FEMS Yeast Res. **7**:604–620.
7. **Boiteux A, Hess B.** 1970. Allosteric properties of yeast pyruvate decarboxylase. FEBS Lett. **9**:293–296.
8. **Boon WR, Calam CT, Gudgeon H, Levi AA.** 1948. Penicillin: analysis of the crude product by partition chromatography. 2. Chromatographic analysis of the penicillins from two strains of *Penicillium notatum*. Biochem. J. **43**:262–265.
9. **Chain E, et al.** 1940. Penicillin as a chemotherapeutic agent. Lancet **ii**:226–228.
10. **Christensen LH, Mandrup G, Nielsen J, Villadsen J.** 1994. A robust liquid chromatographic method for measurement of medium components during penicillin fermentations. Anal. Chim. Acta **296**:51–62.
11. **Committee on Medical Research OSRDW, Medical Research Council.** 1945. Chemistry of penicillin. Science **102**:627–629.
12. **Daran-Lapujade P, Daran JM, van Maris AJ, de Winde JH, Pronk JT.** 2009. Chemostat-based micro-array analysis in baker's yeast. Adv. Microb. Physiol. **54**:257–311.
13. **de Jonge LP, et al.** 2011. Scale-down of penicillin production in *Penicillium chrysogenum*. Biotechnol. J. **6**:944–958.
14. **Douma RD, et al.** 2011. Degeneration of penicillin production in ethanol-limited chemostat cultivations of *Penicillium chrysogenum*: a systems biology approach. BMC Syst. Biol. **5**:132.
15. **Douma RD, et al.** 2010. Intracellular metabolite determination in the presence of extracellular abundance: application to the penicillin biosynthesis pathway in *Penicillium chrysogenum*. Biotechnol. Bioeng. **107**:105–115.
16. **Entian KD, Kötter P.** 2007. Yeast genetic strain and plasmid collections. Methods Microbiol. **36**:629–666.
17. **Fernandez-Canon JM, Penalva MA.** 1995. Fungal metabolic model for human type I hereditary tyrosinaemia. Proc. Natl. Acad. Sci. U. S. A. **92**: 9132–9136.
18. **Fernandez-Canon JM, Penalva MA.** 1995. Molecular characterization of a gene encoding a homogentisate dioxygenase from *Aspergillus nidulans* and identification of its human and plant homologues. J. Biol. Chem. **270**:21199–21205.
19. **Ferrer-Sevillano F, Fernandez-Canon JM.** 2007. Novel phacB-encoded cytochrome P450 monooxygenase from *Aspergillus nidulans* with 3-hydroxyphenylacetate 6-hydroxylase and 3,4-dihydroxyphenylacetate 6-hydroxylase activities. Eukaryot. Cell **6**:514–520.
20. **Fleming A.** 1929. On the antibacterial action of cultures of a *Penicillium*, with special reference to their use in the isolation of *B. influenza*. Exp. Pathol. **10**:226–236.
21. **Flikweert MT, et al.** 1996. Pyruvate decarboxylase: an indispensable enzyme for growth of *Saccharomyces cerevisiae* on glucose. Yeast **12**:247–257.
22. **Gietz RD, Schiestl RH.** 2007. High-efficiency yeast transformation using the LiAc/SS carrier DNA/PEG method. Nat. Protoc. **2**:31–34.
23. **Gombert AK, et al.** 2011. Functional characterization of the oxaloacetase encoding gene and elimination of oxalate formation in the beta-lactam producer *Penicillium chrysogenum*. Fungal Genet. Biol. **48**:831–839.
24. **Gonzalez B, Francois J, Renaud M.** 1997. A rapid and reliable method for metabolite extraction in yeast using boiling buffered ethanol. Yeast **13**: 1347–1355.
25. **Gordon M, Pan S, Virgona A, Numerof P.** 1953. Biosynthesis of penicillin. I. Role of phenylacetic acid. Science **118**:43.
26. **Harris DM, et al.** 2009. Exploring and dissecting genome-wide gene expression responses of *Penicillium chrysogenum* to phenylacetic acid consumption and penicillin G production. BMC Genomics **10**:75–95.
27. **Harris DM, et al.** 2009. Engineering of *Penicillium chrysogenum* for fermentative production of a novel carbamoylated cephem antibiotic precursor. Metab. Eng. **11**:125–137.
28. **Hazelwood LA, Daran JM, van Maris AJA, Pronk JT, Dickinson JR.**

2008. The Ehrlich pathway for fusel alcohol production: a century of research on *Saccharomyces cerevisiae* metabolism. Appl. Environ. Microbiol. **74**:2259–2265.
29. **Hill VA.** 1910. The possible effects of the aggregation of the molecules of hæmoglobin on its dissociation curves. J. Physiol. 40(Suppl.):i-vii.
30. **Hohmann S.** 1991. Characterization of *PDC6*, a third structural gene for pyruvate decarboxylase in *Saccharomyces cerevisiae*. J. Bacteriol. **173**:7963–7969.
31. **Hohmann S, Cederberg H.** 1990. Autoregulation may control the expression of yeast pyruvate decarboxylase structural genes *PDC1* and *PDC5*. Eur. J. Biochem. **188**:615–621.
32. **Hubner G, Weidhase R, Schellenberger A.** 1978. The mechanism of substrate activation of pyruvate decarboxylase: a first approach. Eur. J. Biochem. **92**:175–181.
33. **Juvvadi PR, Seshime Y, Kitamoto K.** 2005. Genomics reveals traces of fungal phenylpropanoid-flavonoid metabolic pathway in the filamentous fungus *Aspergillus oryzae*. J. Microbiol. **43**:475–486.
34. **Kelly JM, Drysdale MR, Sealy-Lewis HM, Jones IG, Lockington RA.** 1990. Alcohol dehydrogenase III in *Aspergillus nidulans* is anaerobically induced and post-transcriptionally regulated. Mol. Gen. Genet. **222**:323–328.
35. **Kishore G, Sugumaran M, Vaidyanathan CS.** 1976. Metabolism of DL-(+/−)-phenylalanine by *Aspergillus niger*. J. Bacteriol. **128**:182–191.
36. **Koetsier MJ, et al.** 2010. The *Penicillium chrysogenum aclA* gene encodes a broad-substrate-specificity acyl-coenzyme A ligase involved in activation of adipic acid, a side-chain precursor for cephem antibiotics. Fungal Genet. Biol. **47**:33–42.
37. **Lange HC, et al.** 2001. Improved rapid sampling for in vivo kinetics of intracellular metabolites in *Saccharomyces cerevisiae*. Biotechnol. Bioeng. **75**:406–415.
38. **Larkin MA, et al.** 2007. Clustal W and Clustal X version 2.0. Bioinformatics **23**:2947–2948.
39. **Lee CJ, Yeh HJ, Yang WY, Kan CR.** 1994. Separation of penicillin G from phenylacetic acid in a supported liquid membrane system. Biotechnol. Bioeng. **43**:309–313.
40. **Lein J.** 1986. The Panlabs penicillin strain improvement program. Biotechnol. Ser. **1986**:105–139.
41. **Lockington RA, Borlace GN, Kelly JM.** 1997. Pyruvate decarboxylase and anaerobic survival in *Aspergillus nidulans*. Gene **191**:61–67.
42. **Lowry O, Rosebrough N, Farr A, Randall R.** 1951. Protein measurement with the Folin phenol reagent. J. Biol. Chem. **193**:265–275.
43. **Lutke-Eversloh T, Stephanopoulos G.** 2005. Feedback inhibition of chorismate mutase/prephenate dehydrogenase (TyrA) of *Escherichia coli:* generation and characterization of tyrosine-insensitive mutants. Appl. Environ. Microbiol. **71**:7224–7228.
44. **Luttik MA, et al.** 2008. Alleviation of feedback inhibition in *Saccharomyces cerevisiae* aromatic amino acid biosynthesis: quantification of metabolic impact. Metab. Eng. **10**:141–153.
45. **Mashego MR, van Gulik WM, Vinke JL, Heijnen JJ.** 2003. Critical evaluation of sampling techniques for residual glucose determination in carbon-limited chemostat culture of *Saccharomyces cerevisiae*. Biotechnol. Bioeng. **83**:395–399.
46. **Mingot JM, Penalva MA, Fernandez-Canon JM.** 1999. Disruption of *phacA*, an *Aspergillus nidulans* gene encoding a novel cytochrome P450 monooxygenase catalyzing phenylacetate 2-hydroxylation, results in penicillin overproduction. J. Biol. Chem. **274**:14545–14550.
47. **Moore K, Rao PV, Towers GH.** 1967. Degradation of phenylalanine and tyrosine by Basidiomycetes. Life Sci. **6**:2629–2633.
48. **Moore K, Rao PV, Towers GH.** 1968. Degradation of phenylalanine and tyrosine by *Sporobolomyces roseus*. Biochem. J. **106**:507–514.
49. **Moore K, Towers GH.** 1967. Degradation of aromatic amino acids by fungi. I. Fate of L-phenylalanine in *Schizophyllum commune*. Can. J. Biochem. **45**:1659–1665.
50. **Moyer AJ, Coghill RD.** 1946. Penicillin: IX. The laboratory scale production of penicillin in submerged cultures by *Penicillium notatum* Westling (NRRL 832). J. Bacteriol. **51**:79.
51. **Moyer AJ, Coghill RD.** 1946. Penicillin: VIII. Production of penicillin in surface cultures. J. Bacteriol. **51**:57.
52. **Moyer AJ, Coghill RD.** 1947. Penicillin: X. The effect of phenylacetic acid on penicillin production. J. Bacteriol. **53**:329–341.
53. **Mumberg D, Muller R, Funk M.** 1995. Yeast vectors for the controlled expression of heterologous proteins in different genetic backgrounds. Gene **156**:119–122.
54. **Nasution U, van Gulik WM, Proell A, van Winden WA, Heijnen JJ.** 2006. Generating short-term kinetic responses of primary metabolism of *Penicillium chrysogenum* through glucose perturbation in the bioscope mini reactor. Metab. Eng. **8**:395–405.
55. **Newbert RW, Barton B, Greaves P, Harper J, Turner G.** 1997. Analysis of a commercially improved *Penicillium chrysogenum* strain series: involvement of recombinogenic regions in amplification and deletion of the penicillin biosynthesis gene cluster. J. Ind. Microbiol. Biotechnol. **19**:18–27.
56. **Noh K, Wahl A, Wiechert W.** 2006. Computational tools for isotopically in stationary 13C labeling experiments under metabolic steady state conditions. Metab. Eng. **8**:554–577.
57. **Owen S, Johnson M.** 1955. The effect of temperature changes on the production of penicillin by *Penicillium chrysogenum* W49-133. Appl. Microbiol. **3**:375–379.
58. **Packer HL, Keshavarz-Moore E, Lilly MD, Thomas CR.** 1992. Estimation of cell volume and biomass of *Penicillium chrysogenum* using image analysis. Biotechnol. Bioeng. **39**:384–391.
59. **Perlman D.** 1966. Chemically defined media for antibiotic production. Ann. N. Y. Acad. Sci. **139**:258–269.
60. **Postma E, Verduyn C, Scheffers WA, Van Dijken JP.** 1989. Enzymic analysis of the crabtree effect in glucose-limited chemostat cultures of *Saccharomyces cerevisiae*. Appl. Environ. Microbiol. **55**:468–477.
61. **Rodriguez-Saiz M, et al.** 2001. Reduced function of a phenylacetate-oxidizing cytochrome p450 caused strong genetic improvement in early phylogeny of penicillin-producing strains. J. Bacteriol. **183**:5465–5471.
62. **Rodriguez-Saiz M, Diez B, Barredo JL.** 2005. Why did the Fleming strain fail in penicillin industry? Fungal Genet. Biol. **42**:464–470.
63. **Sambrook J, Fritsch E, Maniatis T.** 1989. Molecular cloning: a laboratory manual. Cold Spring Harbor Laboratory Press, Cold Spring Harbor, NY.
64. **Schull TL, Fettinger JC, Knight DA.** 1996. Synthesis and characterization of palladium(II) and platinum(II) complexes containing water-soluble hybrid phosphine-phosphonate ligands. Inorg. Chem. **35**:6717–6723.
65. **Seshime Y, Juvvadi PR, Fujii I, Kitamoto K.** 2005. Genomic evidences for the existence of a phenylpropanoid metabolic pathway in *Aspergillus oryzae*. Biochem. Biophys. Res. Commun. **337**:747–751.
66. **Singh K, Johnson MJ.** 1948. Evaluation of precursors for penicillin G. J. Bacteriol. **56**:339–355.
67. **Skory CD.** 2003. Induction of *Rhizopus oryzae* pyruvate decarboxylase genes. Curr. Microbiol. **47**:59–64.
68. **Snoek IS, et al.** 2009. Construction of an *hdfA Penicillium chrysogenum* strain impaired in non-homologous end-joining and analysis of its potential for functional analysis studies. Fungal Genet. Biol. **46**:418–426.
69. **Stone RW, Farrell MA.** 1946. Synthetic media for penicillin production. Science **104**:445–446.
70. **Tusher VG, Tibshirani R, Chu G.** 2001. Significance analysis of microarrays applied to the ionizing radiation response. Proc. Natl. Acad. Sci. U. S. A. **98**:5116–5121.
71. **van den Berg MA, et al.** 2008. Genome sequencing and analysis of the filamentous fungus *Penicillium chrysogenum*. Nat. Biotechnol. **26**:1161–1168.
72. **van Gulik WM, de Laat WT, Vinke JL, Heijnen JJ.** 2000. Application of metabolic flux analysis for the identification of metabolic bottlenecks in the biosynthesis of penicillin-G. Biotechnol. Bioeng. **68**:602–618.
73. **Verduyn C, Postma E, Scheffers WA, Van Dijken JP.** 1992. Effect of benzoic acid on metabolic fluxes in yeasts: a continuous-culture study on the regulation of respiration and alcoholic fermentation. Yeast **8**:501–517.
74. **Vuralhan Z, et al.** 2005. Physiological characterization of the ARO10-dependent, broad-substrate-specificity 2-oxo acid decarboxylase activity of *Saccharomyces cerevisiae*. Appl. Environ. Microbiol. **71**:3276–3284.
75. **Vuralhan Z, Morais MA, Tai SL, Piper MD, Pronk JT.** 2003. Identification and characterization of phenylpyruvate decarboxylase genes in *Saccharomyces cerevisiae*. Appl. Environ. Microbiol. **69**:4534–4541.
76. **Wahl SA, Dauner M, Wiechert W.** 2004. New tools for mass isotopomer data evaluation in ^{13}C flux analysis: mass isotope correction, data consistency checking, and precursor relationships. Biotechnol. Bioeng. **85**:259–268.
77. **White S, Berry DR, McNeil B.** 1999. Effect of phenylacetic acid feeding on the process of cellular autolysis in submerged batch cultures of *Penicillium chrysogenum*. J. Biotechnol. **75**:173–185.
78. **Wu L, et al.** 2005. Quantitative analysis of the microbial metabolome by isotope dilution mass spectrometry using uniformly ^{13}C-labeled cell extracts as internal standards. Anal. Biochem. **336**:164–171.